9-1-2016

Interplay of brain structure and function in neonatal congenital heart disease

Ala Birca
Hospital for Sick Children University of Toronto

Vasily A. Vakorin
Simon Fraser University

Prashob Porayette
Hospital for Sick Children University of Toronto

Sujana Madathil
SickKids Research Institute

Vann Chau
Hospital for Sick Children University of Toronto

See next page for additional authors

ANNALS of Clinical and Translational Neurology
Open Access
ANA American Neurological Association since 1875

RESEARCH ARTICLE

Interplay of brain structure and function in neonatal congenital heart disease

Ala Birca[1,2], Vasily A. Vakorin[3], Prashob Porayette[4], Sujana Madathil[5], Vann Chau[1,5], Mike Seed[4,5], Sam M. Doesburg[3], Susan Blaser[5,6], Dragos A. Nita[1,5], Rohit Sharma[1], Emma G. Duerden[5], Edward J. Hickey[5,7], Steven P. Miller[1,5,a] & Cecil D. Hahn[1,5,a]

[1]Division of Neurology, Department of Paediatrics, The Hospital for Sick Children and the University of Toronto, Toronto, Canada
[2]Division of Neurology, Department of Neuroscience, CHU Sainte-Justine and the University of Montreal, Montreal, Canada
[3]Department of Biomedical Physiology and Kinesiology, Simon Fraser University, Burnaby, Canada
[4]Division of Cardiology, Department of Paediatrics, The Hospital for Sick Children and the University of Toronto, Toronto, Canada
[5]Program in Neurosciences and Mental Health, SickKids Research Institute, Toronto, Canada
[6]Department of Diagnostic Imaging, The Hospital for Sick Children, Toronto, Canada
[7]Division of Cardiovascular Surgery, Department of Surgery, The Hospital for Sick Children and the University of Toronto, Toronto, Canada

Correspondence
Cecil D. Hahn, Division of Neurology, The Hospital for Sick Children, 555 University Avenue, Toronto, Ontario, Canada M5G 1X8. Tel: 416-813-7037; Fax: 416-813-6334; E-mail: cecil.hahn@sickkids.ca

Funding Information
This study was supported by the Canadian Institutes of Health Research (CIHR) Operating Grant to S. P. M. (MOP93780), as well as the CHU Sainte-Justine/Group Aldo scholarship and Detweiler Travelling Fellowship from the RCPSC (Royal College of Physicians and Surgeons of Canada) to A. B. S. P. M. is supported by the Bloorview Children's Hospital Chair in Paediatric Neuroscience.

Received: 25 June 2016; Accepted: 5 July 2016

Annals of Clinical and Translational Neurology **2016; 3(9): 708–722**

doi: 10.1002/acn3.336

[a]These authors contributed equally to this work.

Abstract

Objective: To evaluate whether structural and microstructural brain abnormalities in neonates with congenital heart disease (CHD) correlate with neuronal network dysfunction measured by analysis of EEG connectivity. **Methods**: We studied a prospective cohort of 20 neonates with CHD who underwent continuous EEG monitoring before surgery to assess functional brain maturation and network connectivity, structural magnetic resonance imaging (MRI) to determine the presence of brain injury and structural brain development, and diffusion tensor MRI to assess brain microstructural development. **Results**: Neonates with MRI brain injury and delayed structural and microstructural brain development demonstrated significantly stronger high-frequency (beta and gamma frequency band) connectivity. Furthermore, neonates with delayed microstructural brain development demonstrated significantly weaker low-frequency (delta, theta, alpha frequency band) connectivity. Neonates with brain injury also displayed delayed functional maturation of EEG background activity, characterized by greater background discontinuity. **Interpretation**: These data provide new evidence that early structural and microstructural developmental brain abnormalities can have immediate functional consequences that manifest as characteristic alterations of neuronal network connectivity. Such early perturbations of developing neuronal networks, if sustained, may be responsible for the persistent neurocognitive impairment prevalent in adolescent survivors of CHD. These foundational insights into the complex interplay between evolving brain structure and function may have relevance for a wide spectrum of neurological disorders manifesting early developmental brain injury.

Introduction

Brain development involves the precise refinement of brain structure in response to nascent brain activity. Structural alterations are known to disrupt this process, leading to neuronal network dysfunction that may underlie persistent neurocognitive deficits.[1,2] However, the ability to predict such neurocognitive deficits remains limited, and the relationship between structural neuroimaging abnormalities and neuronal network dysfunction remains poorly understood.

Congenital heart disease (CHD) provides a remarkable model to examine how structural brain alterations impact functional network development. Term neonates with CHD demonstrate abnormal structural brain development, with delayed cortical folding and myelination.[3] Furthermore, their brain microstructure, assessed using diffusion tensor imaging (DTI), is also delayed, similar to

findings in premature neonates ~1 month before term.[4] This dysmaturation or delayed brain structure and microstructure likely reflect their exquisite vulnerability to white matter injury (WMI), a pattern of injury characteristic of the preterm neonate and occurring in 20–50% of term neonates with CHD before and after the surgery.[5,6] Identifying early functional correlates of the observed neuroimaging abnormalities would reveal whether structural and microstructural abnormalities have functional consequences, and whether early neuronal network dysfunction may be responsible for persistent cognitive deficits, observed in more than half of survivors of CHD.[7]

EEG background activity has long been recognized as a robust measure of functional brain maturation and impairment.[8] Neonates with CHD demonstrate abnormal maturation of EEG background patterns, as assessed using amplitude EEG before surgery.[9] Furthermore, quantitative EEG analysis has shown lower frontal beta frequency power in neonates with CHD who experienced worse cognitive outcome at 18 months of age.[10] EEG connectivity is also increasingly used to assess functional maturation.[11] This novel approach offers an unprecedented opportunity to study, at the bedside, neuronal network functioning and understand how structural magnetic resonance imaging (MRI) abnormalities such as those observed in CHD interfere with network development.

In this study, we evaluate the hypothesis that structural and microstructural brain abnormalities in neonates with CHD correlate with neuronal network dysfunction measured by analysis of EEG connectivity. We studied a prospective cohort of neonates with CHD who underwent continuous EEG monitoring (cEEG) before surgery to assess functional brain maturation and network connectivity, structural MRI to determine the presence of brain injury and structural brain development, and diffusion tensor MRI to assess brain microstructural development. Our main objective was to investigate the association between EEG connectivity and the following structural brain parameters: (1) the presence of brain injury on MRI, (2) structural brain maturation as assessed using the total maturation score (TMS)[3] and (3) white matter microstructural development as assessed using DTI. Moreover, considering previous EEG findings in neonates with CHD, we also assessed the association between these structural brain parameters with (1) EEG background development and (2) EEG spectral power.

Methods

Subjects

Between July 2013 and March 2015, we prospectively enrolled a cohort of 33 near-term neonates (>36 weeks postmenstrual age [PMA]) with CHD, transferred to The Hospital for Sick Children, a regional tertiary level cardiac referral center. Neonates were eligible for study participation if heart surgery was planned within the first 3 months of life. They were excluded if a congenital infection or genetic malformation syndrome was diagnosed or suspected. During the study period, 20 of the 33 enrolled neonates were included in this study. The 13 neonates who were excluded were either too medically unstable to participate, or consent could not be obtained for preoperative MRI ($n = 3$), cEEG ($n = 5$) or both ($n = 5$). All participating neonates underwent preoperative cEEG recordings. Eighteen of them also underwent preoperative MRI scans, all within 6 days of cEEG (median 2 days). DTI data were acquired in only 11 of 18 neonates with preoperative scans, owing to excessive motion or inability to complete the study due to clinical factors.

Clinical data were prospectively collected from the medical records and are summarized in Table 1. The research ethics board of The Hospital for Sick Children approved the study protocol and the parents of all participating neonates provided written informed consent.

MRI evaluations

MRI studies were performed both preoperatively and postoperatively, according to a standard protocol (see

Table 1. Clinical characteristics of the neonates with CHD.

Characteristic	Frequency or median
Male sex, *n*	9 (45)
Prenatal diagnosis, *n*	19 (95)
Cesarean delivery, *n*	6 (30)
Gestational age at birth, weeks	38.9 (38.4–39.6)
Birth weight, kg	3.4 (3.1–3.5)
Birth head circumference, cm	35 (33.8–35.6)
Apgar score at 5 min	9 (8–9)
Resuscitation score[1]	0 (0–1)
Heart lesion	
Transposition of the great arteries, *n*	10 (50)
Single-ventricle physiology, *n*	6 (30)
Left heart obstructive lesion, *n*	3 (15)
Right-sided lesion, *n*	1 (5)
Preoperative mechanical ventilation, *n*	5 (25)
Preoperative inotropic support, *n*	4 (20)
Prostaglandin E_1, *n*	20 (100)
Balloon atrial septostomy, *n*	7 (35)
Preoperative MRI postmenstrual age, weeks	39.4 (39–40.3)
Preoperative cEEG postmenstrual age, weeks	39.5 (38.8–40.5)

Data are presented as *n* (%) or median (interquartile range). CHD, congenital heart disease; MRI, magnetic resonance imaging; cEEG, continuous EEG.

[1]The resuscitation score is based on interventions that are administered at birth, ranging from 1 (no intervention) to 6 (endotracheal intubation and epinephrine).[14]

Data S1), as soon as neonates could be safely transported by trained personnel to a 1.5T Avanto Scanner (Siemens Medical Systems, Erlangen, Germany) with syngo MR B17.

Only preoperative MRI assessments were used in this study, except for two neonates. These two neonates had only postoperative MRI scans, but we included them in the group of patients without brain injury because their preoperative head ultrasound and postoperative MRI scans were normal. Their brain maturation (TMS) and microstructure (DTI) were not assessed in this study.

Preoperative MRI assessments were performed without sedation, except for one neonate who was under general anesthesia for clinical assessment. No adverse events occurred during this protocol.

Assessment of brain injury

A neuroradiologist (S. B.) who was unaware of any clinical information except age and cardiac diagnosis examined the diffusion, T1- and T2-weighted sequences for acquired injury and developmental brain abnormalities. Brain injury was characterized as stroke, WMI, intraventricular hemorrhage, or global hypoxic-ischemic injury, as reported previously.[12,13]

Assessment of structural brain maturation

We used the TMS[3] to quantify structural brain maturation. Scoring was performed by a neuroradiologist (S. B.) who was unaware of any clinical data except age and cardiac diagnosis. Axial T1- and T2-weighted images were used to evaluate four parameters of maturity: (1) myelination (average of scores obtained separately on T1 and T2 images for each hemisphere), (2) cortical infolding (average of individual scores obtained for frontal/occipital and insular cortex), (3) involution of glial cell migration bands, and (4) presence of germinal matrix tissue. Scores were then added to obtain the final TMS, which is known to increase with PMA up to a maximum of 19.5 points.

DTI of white matter microstructure

DTI provides a sensitive measure of regional brain microstructure. It characterizes the 3D spatial distribution of water diffusion permitting quantification of two complementary measures: average diffusivity (D_{av}) and fractional anisotropy (FA). D_{av} represents the magnitude of water diffusion in brain tissue, which decreases with white matter maturation due to the development of neuronal and glial cell membranes that restrict water diffusion. FA is a measure of the degree of directionality of water diffusion, which increases with white matter maturation, particularly due to the maturation of the oligodendrocyte lineage and early events of myelination.[14,15] D_{av} and FA were calculated from five white matter regions of interest drawn manually and bilaterally: frontal, perirolandic, posterior white matter at the level of centrum semiovale, and frontal and posterior deep white matter.[4]

EEG evaluations

Continuous video-EEG recordings lasting ~24 h were acquired using portable Stellate Vita ICU video-EEG systems (Natus Neurology, Oakville, Ontario, Canada), with a sampling rate of 200 Hz and a 0.1–100 Hz band pass filter. Electrodes were applied by registered EEG technologists according to the International 10–20 system of electrode placement modified for neonates (Fp1, C3, T3, O1, M1, Fp2, C4, T4, O2, M2, Fz, Cz, and Pz, all referenced to a system reference electrode Pz'). All neonates had a simultaneous recording of deltoid electromyogram, electrocardiogram, and abdominal respiration. Only one neonate, without brain injury, received low doses of sedative medication (morphine) during the recording. One neonate had seizures that started 3.5 h after the beginning of the cEEG recording, but received antiepileptic medication only after the end of the 4-h period subjected to analysis.

Visual analysis of EEG background activity

All recordings were interpreted by board-certified clinical neurophysiologists (A. B. and C. D. H.). The first 4 h of EEG recordings were visually inspected and consecutive EEG epochs were manually marked and classified according to accepted criteria[16] into one of four EEG background patterns (see Data S2): (1) awake/active sleep, (2) transitional/high-voltage sleep, (3) *tracé alternant* and (4) *tracé discontinu*. The whole 4-h period was manually marked for each neonate and the percentage of recording time corresponding to each EEG background pattern was quantified. On a few occasions, reliable categorization of the EEG background pattern was complicated by artifacts from concomitant infant care, procedures or the occurrence of electrographic seizures, in which case these EEG epochs were skipped and additional successive epochs of identical duration were included in the analysis.

Computational EEG analysis

Preprocessing

Similar to visual analysis, computational analysis was performed on the first 4 h of EEG recordings, focusing on continuous background activity. Separately for each subject, EEG epochs corresponding to the awake/active

sleep pattern or transitional/high-voltage sleep pattern were divided into nonoverlapping 20-sec EEG segments. Segments without any movement, ocular, muscle or other artifact were exported, using the Stellate-Harmonie Toolbox for MATLAB (courtesy J. Gotman) for further analysis (awake/active sleep: mean 97 ± 43 segments/subject, range 34–176; transitional/high-voltage sleep: mean 92 ± 58 segments/subject, range 31–286). EEG recordings were then band-pass filtered (1–55 Hz), using a Hamming windowed finite-impulse response filter[17] and re-referenced to linked mastoid electrodes, resulting in 11 active scalp electrodes available for analysis.

Computation of connectivity

Connectivity was estimated by computing the phase synchrony between pairs of electrodes. To obtain phase dynamics, the time-frequency representation of the original electrode dynamics was derived from wavelet decomposition.[18] Specifically, we used a time-frequency toolbox,[19] estimating amplitude and phase dynamics of EEG activity at 30 frequency points equally spaced on a logarithmic scale between 1 and 55 Hz. Phase synchrony was then quantified as frequency-specific phase locking between the instantaneous phases of two signals, producing the weighted phase lag index (wPLI) on a pair-wise basis.[20] Thus, thirty 11 × 10/2 matrices were generated for each segment and each subject, representing phase synchrony between all the combinations of 11 EEG electrodes at 30 frequency points, and then averaged across segments.

Computation of spectral power density

Spectral power density for each time series (each segment, subject, and electrode) was estimated with a step of 1 Hz by Welch's time-averaged, modified periodogram method,[21] with a subsequent averaging across segments, separately for each subject and each electrode. Given the sampling rate of 200 Hz, the analysis was constrained to the 1–55 Hz range, covering canonical frequency bands from delta to lower gamma: delta (1–3.5 Hz), theta (3.5–8 Hz), alpha (8–13 Hz) beta (13–30 Hz) and low gamma (30–55 Hz).

Statistical analyses

We performed multivariate analyses to investigate the association between brain function (EEG connectivity, spectral power density and background pattern), and brain structure (presence of brain injury, TMS, and DTI measures).

We applied Partial Least Squares (PLS) analysis, a multivariate technique that operates on the entire data structure at once with the data organized into matrices,[22,23] to examine the covariance between EEG parameters and brain structure matrices (see Data S3). Before PLS, we removed linear PMA-related trends, if any, from EEG, DTI measures and TMS scores. To appreciate the association between EEG parameters and brain injury, we calculated the group contrasts between neonates with and without brain injury, while overall correlations were calculated to appreciate the covariance between EEG parameters and TMS or DTI matrices (panels A of the Figs. 1–6). Group contrasts or correlations were calculated for every element included in the EEG spectral power (11 × 55, electrodes × frequencies) or connectivity matrices (11 × 10/2 unique electrode pairs × 30 frequency points). The contribution of each element was then appreciated using *z*-scores, with values larger than 2.5 (positive or negative) indicating robust effects (panels B of the Figs. 1–6). For each analysis, we report the overall *P*-values and the maps of the *z*-scores illustrating how the tested contrasts or correlations were expressed across EEG frequencies (panels C of Figs. 1–6 and panels D of Figs. 5, 6) and connections (topographic plots in Figs. 1–6).

Finally, linear regression analyses, with adjustment for PMA, were used to investigate whether the presence of brain injury or the TMS scores predict the percentages of recording time corresponding to each EEG pattern.

Results

Clinical characteristics

Acquired brain injury was detected on preoperative MRI in 5 (25%) of 20 neonates: four with WMI and one with combined white and gray matter injury. Transposition of the great arteries (TGA) was the most frequent cardiac diagnosis (Table 1), encountered in 10 of 20 neonates and associated with acquired brain injury in three of them (30%). Neonates with and without TGA had similar TMS scores (13.4 ± 0.9 vs. 13.8 ± 0.7, respectively). Nineteen of 20 neonates had cardiac surgery (median 7 days after birth, range 2–46 days, except one at 3.5 months after birth). One neonate had an improvement in his cardiac condition and no surgery was planned at the time of his 4-month follow-up.

Neonates included in the study were representative of the whole population of CHD neonates in this cohort. Included and excluded patients were similar with respect to PMA, cardiac diagnoses, and the frequency of brain injury detected on the postoperative MRI (46% and 50%, respectively).

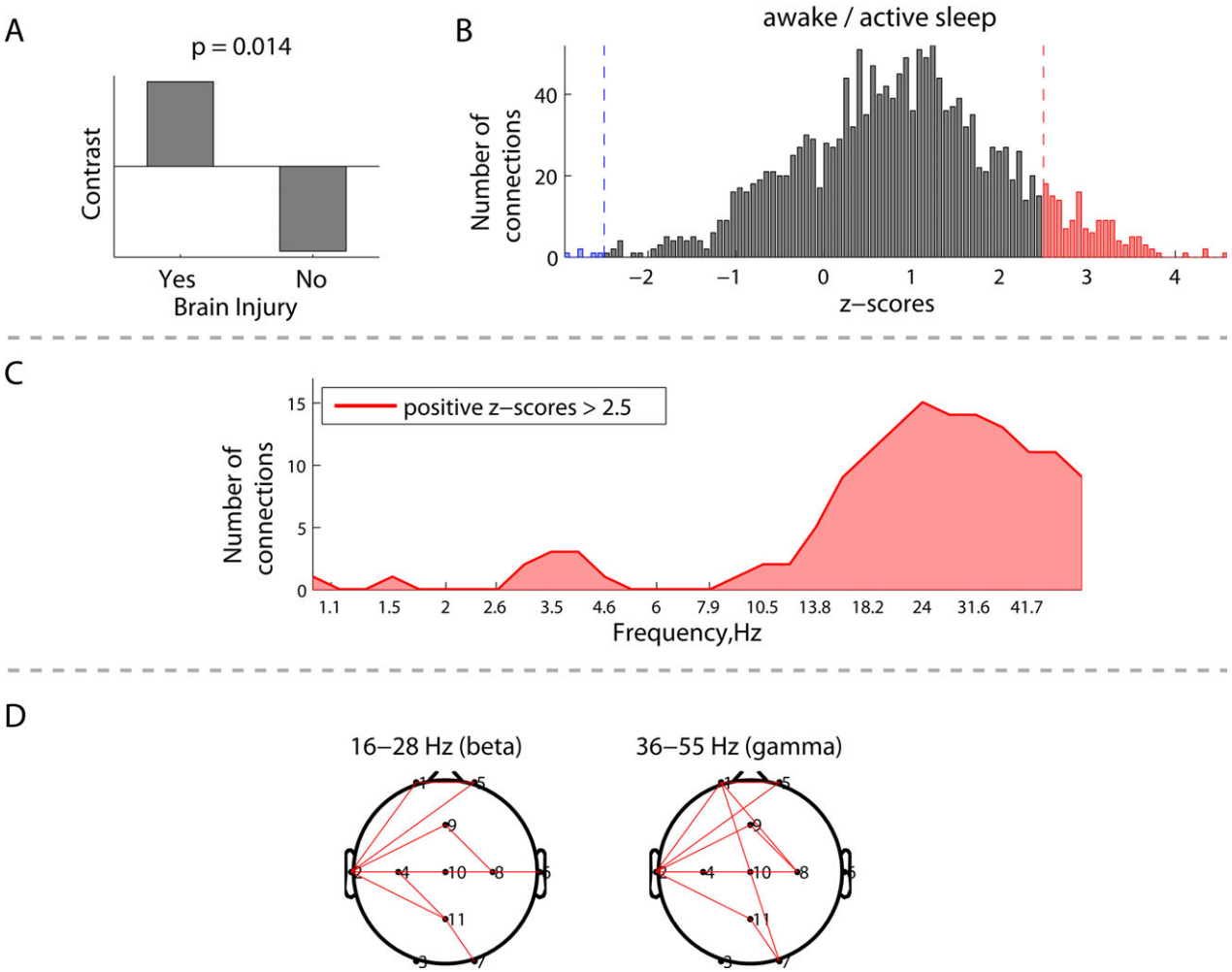

Figure 1. Group differences in EEG connectivity during awake/active sleep between neonates with (N = 5) and without brain injury (N = 15): (A) group contrast; (B) overall distribution of all the z-scores, each associated with a unique combination of frequencies and connections, and showing the robustness of the contrast (A); (C) frequency-dependent distribution of connections from the positive tail (red) of the distribution (B), representing significantly higher phase synchronization between the electrodes for the neonates with brain injury; and (D) spatial distributions of the connections from (C) in the beta and gamma frequency bands.

EEG connectivity

EEG connectivity and brain injury

The presence of brain injury in neonates with CHD was associated with increased EEG connectivity, which was preferentially expressed in the beta/gamma frequency range. Figures 1 and 2 depict the group differences in EEG connectivity between neonates with and without brain injury. Significant between-group contrasts (Figs. 1A, 2A) were evident during both awake/active sleep (P = 0.014) and transitional/high-voltage sleep (P = 0.048). In both cases, the distribution of z-scores was skewed toward the positive tail (Figs. 1B, 2B), indicating that, on average, EEG connectivity was greater among neonates with brain injury. Focusing on the strongest effects, defined by the threshold of 2.5 and −2.5 for z-scores (which is approximately equivalent to the 95% confidence interval), Figures 1C and 2C depict the number of significant connections (electrode pairs) related to each EEG frequency. During awake/active sleep, the number of significant connections was greatest in the beta/gamma frequency band. This pattern was also seen during transitional/high-voltage sleep, with an additional (weaker) effect seen at delta and theta frequencies.

EEG connectivity and structural brain maturation

Immature brain structure (lower TMS score) was associated with increased beta frequency EEG connectivity. Figures 3A and 4A demonstrate significant correlations between EEG connectivity and TMS during both awake/

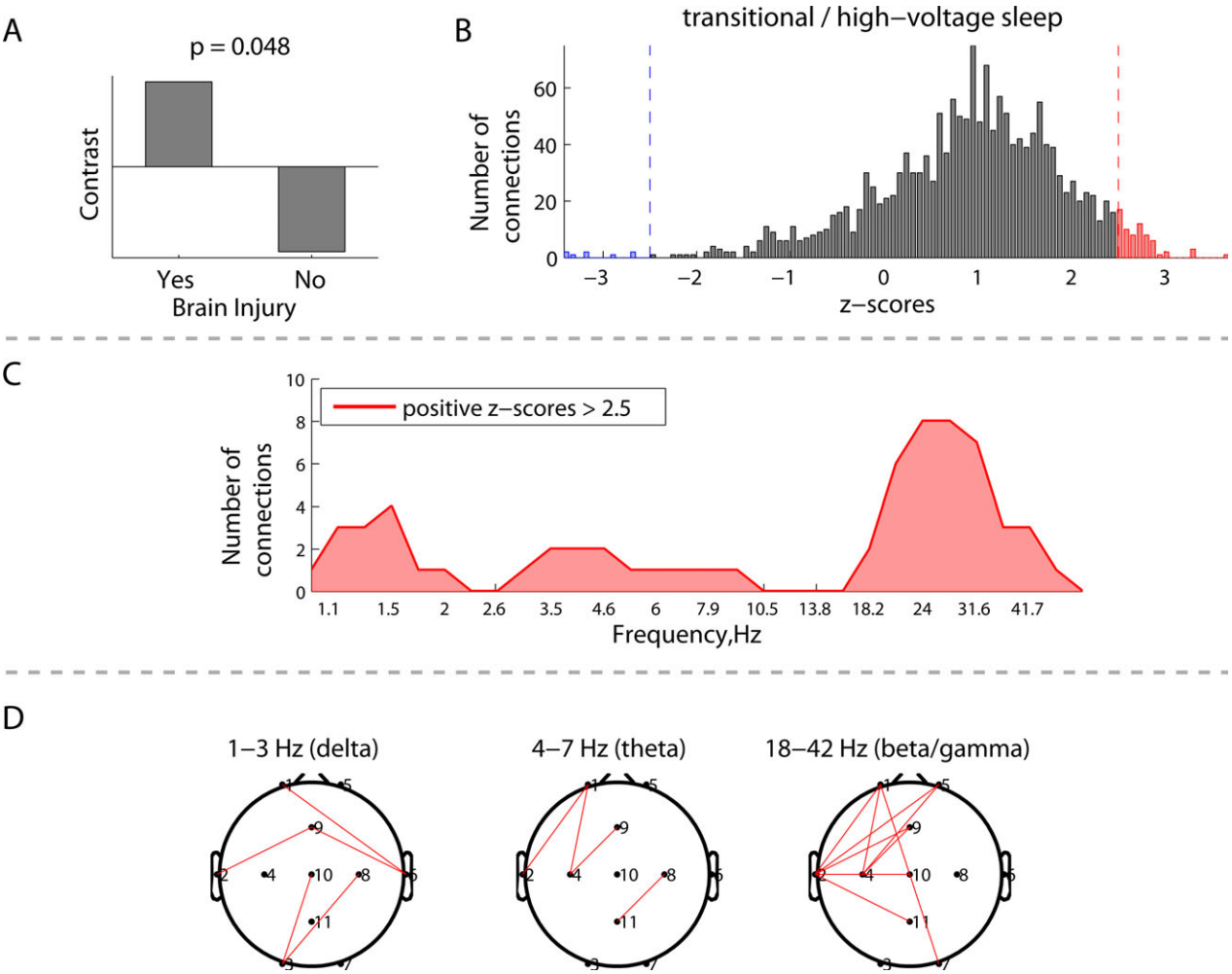

Figure 2. Group differences in EEG connectivity during transitional/high-voltage sleep between neonates with (N = 5) and without brain injury (N = 15): (A) group contrast; (B) overall distribution of all the z-scores, each associated with a unique combination of frequencies and connections, and showing the robustness of the contrast (A); (C) distribution of connections from the positive tail (red) in (B) across frequencies, representing significantly higher phase synchronization between the electrodes for the neonates with brain injury; and (D) spatial distributions of the connections from (C) at the delta, theta, and beta/gamma frequencies.

active sleep (P = 0.01) and transitional/high-voltage sleep (P = 0.004). The distribution of z-scores (Figs. 3B, 4B) was skewed toward negative values (blue), indicating that, on average, lower TMS scores correlated with greater EEG connectivity. Focusing on these strong negative correlations, Figures 3C and 4C illustrate that the number of significant connections is greatest in the beta frequency band. The corresponding spatial distributions of these significant connections are illustrated in Figures 3D and 4D.

EEG connectivity and white matter microstructure

Immature white matter microstructure characterized by low FA was associated with increased high-frequency connectivity (high beta and gamma), but decreased connectivity at lower frequencies (delta, theta, alpha and low beta). This association was not significant during the awake/active sleep (P = 0.068), but attained significance during the transitional/high-voltage sleep (P = 0.014), as shown in Figures 5 and 6 respectively. The panels A show that the contributions of individual white matter regions to the covariance between the two matrices were qualitatively similar.

During transitional/high-voltage sleep (Fig. 6B), the distribution of z-scores revealed equally evident right and left tails, corresponding to positive and negative correlations between EEG connectivity and FA, respectively. Focusing on the positive correlations, Figure 6C depicts a greater number of significant connections supported by low frequencies (delta, theta, alpha, and low beta). Conversely,

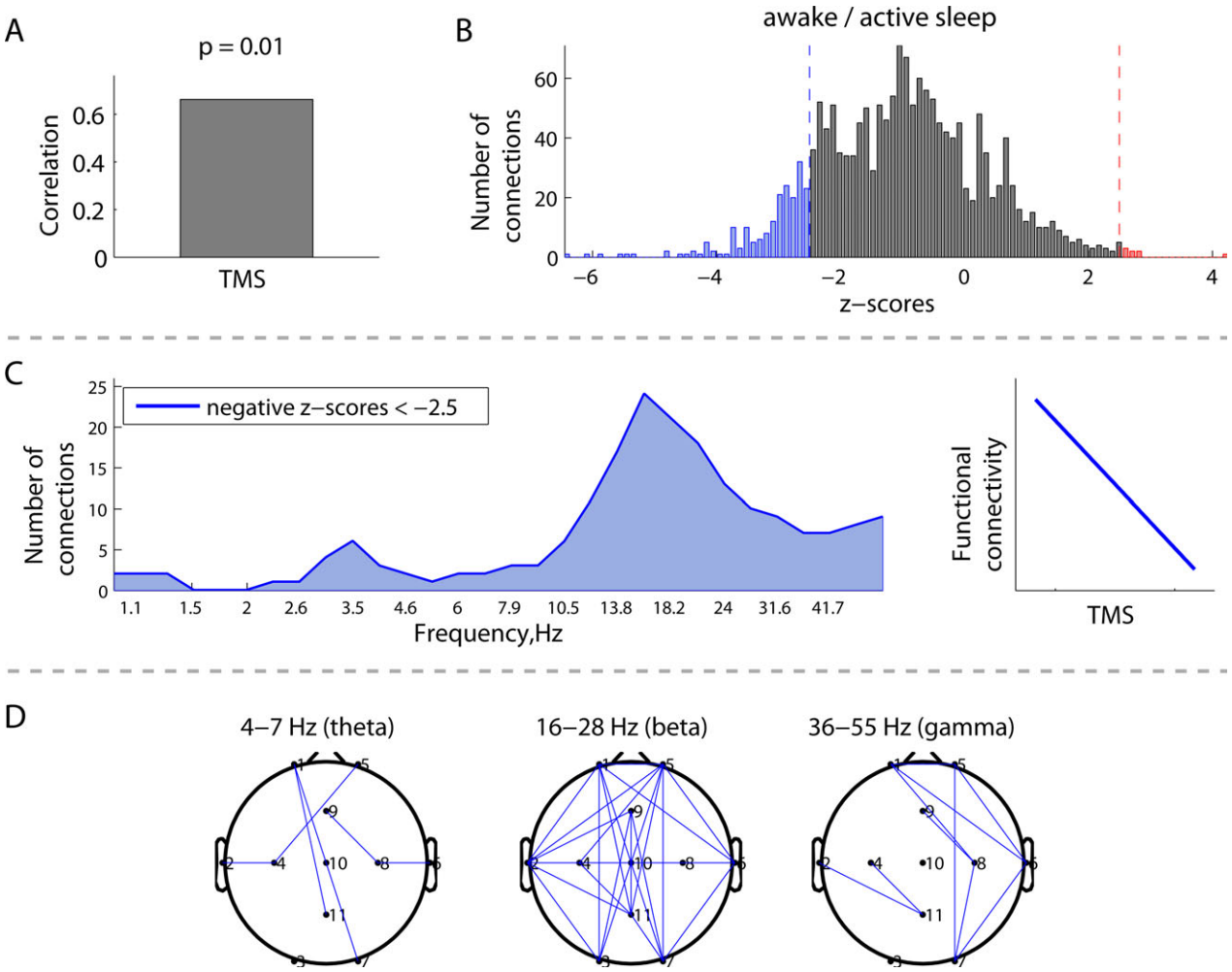

Figure 3. Correlations between EEG connectivity during awake/active sleep and structural brain maturation measured by total maturation score (TMS) (N = 18): (A) overall correlation; (B) distribution of all the z-scores, which show the robustness of the correlation for all possible combinations of frequencies and connections; (C) distribution of connections from the negative tail in (B) across frequencies, associated with a robust negative correlation between EEG connectivity and TMS, as schematically illustrated at the right; and (D) spatial patterns of the correlations between EEG connectivity and TMS in the theta, beta, and gamma frequency bands.

negative correlations were expressed at higher frequencies (high beta and gamma, Fig. 6D). Positive correlations indicated that, on average, high (mature) FA was associated with increased EEG connectivity, whereas low (immature) FA was associated with decreased EEG connectivity, predominantly at lower frequencies. Negative correlations indicated that, on average, low FA was associated with increased connectivity at higher frequencies.

During the awake/active sleep state (Fig. 5B), the distribution of z-scores was skewed toward the right tail, corresponding to positive correlations between EEG connectivity and FA. Although the overall association was not significant (P = 0.068), Figure 5C demonstrates an increased number of connections with significant positive correlations in the alpha and low beta frequency bands. Similar to during transitional/high-voltage sleep, positive correlations indicated that, on average, high (mature) FA was associated with increased EEG connectivity, whereas low (immature) FA was associated with decreased EEG connectivity at alpha and low beta frequencies. The corresponding spatial distributions of these patterns are illustrated in Figures 5E and 6E.

We found no significant associations between white matter D_{av} and EEG connectivity during awake/active sleep (P = 0.25) and transitional/high-voltage sleep (P = 0.6).

EEG spectral power density

We found no significant associations between EEG spectral power density and brain injury, brain maturation (TMS score), or brain microstructure (white matter FA and D_{av}).

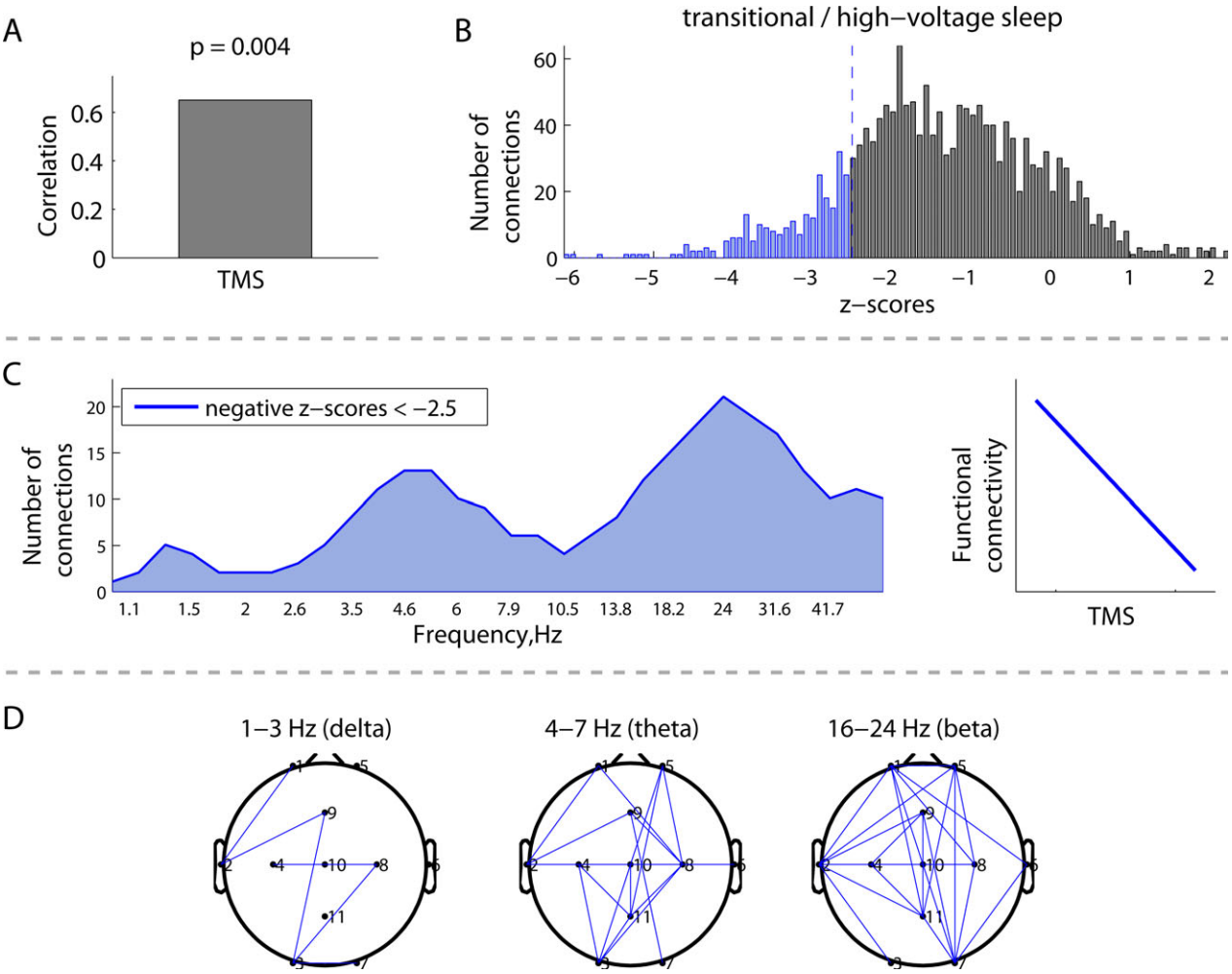

Figure 4. Correlations between EEG connectivity during transitional/high-voltage sleep and structural brain maturation measured by total maturation score (TMS) ($N = 18$): (A) overall correlation; (B) distribution of all the *z*-scores, showing the robustness of the correlation for all possible combinations of frequencies and connections; (C) distribution of connections from the negative tail in (B) across frequencies, associated with a robust negative correlation between connectivity and TMS, as schematically illustrated at the right; and (D) spatial patterns of the correlations between EEG connectivity and TMS in the delta, theta, and beta frequency bands.

EEG background pattern

As expected, younger PMA was associated with significantly less time spent in awake/active sleep and more time in transitional/high-voltage sleep and *tracé discontinu* EEG background patterns ($P < 0.05$, Fig. 7). However, when PMA was entered into a multiple regression model together with brain injury, only brain injury remained significantly associated with EEG background pattern. As illustrated in Figure 7, after adjusting for PMA, we found that neonates with brain injury spent significantly less time in the continuous EEG background pattern of awake/active sleep ($F_{2;17} = 10.5$, $P = 0.001$) and significantly more time in the discontinuous EEG background patterns *tracé alternant* ($F_{2;17} = 7.3$, $P = 0.005$) and *tracé discontinu* ($F_{2;17} = 9.3$, $P = 0.002$).

We found no significant association between EEG background pattern and brain maturation (TMS score) or brain microstructure (white matter FA and D_{av}).

Discussion

This study provides new evidence that early structural and microstructural developmental brain abnormalities in neonates with CHD can have immediate functional consequences that manifest as characteristic alterations of neuronal network connectivity. Specifically, abnormal brain structure and microstructure exert opposite effects

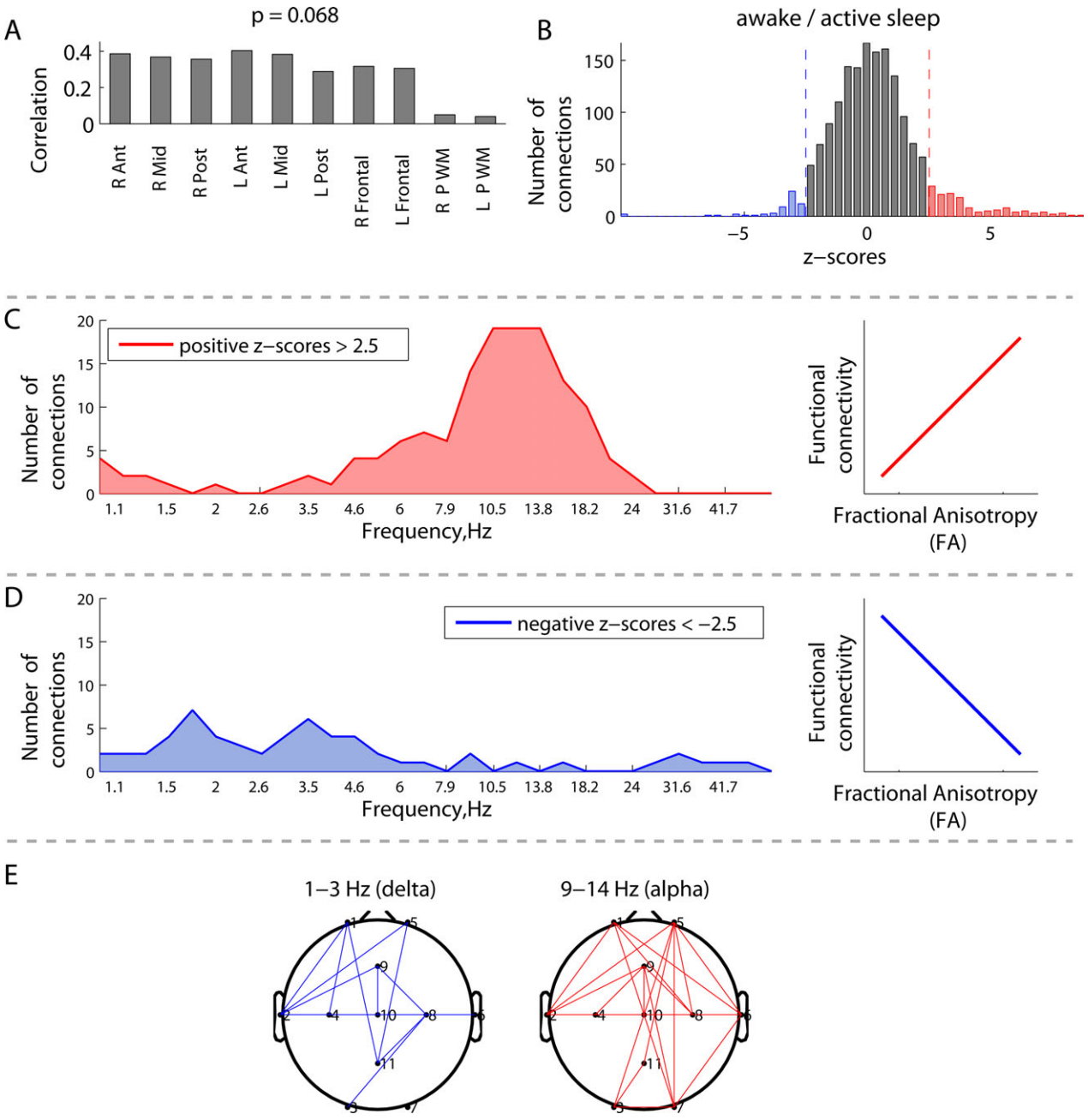

Figure 5. Correlations between EEG connectivity during awake/active sleep and white matter fractional anisotropy (FA) (N = 11): (A) overall correlations between white matter FA at 10 specific regions of interest and EEG connectivity; (B) distribution of the z-scores, each associated with a unique combination of frequencies and connections, and showing the robustness of the latent variable in (A); (C) distribution of connections from the positive tail (red) in (B) across frequencies, associated with a robust positive correlation between EEG connectivity and FA, as schematically illustrated at the right; (D) distribution of the connections from the negative tail (blue) in (B), associated with a robust negative correlation between EEG connectivity and FA; (E) spatial patterns of the correlations between EEG connectivity and FA at the delta and alpha frequency peaks defined by the distributions in (C and D).

on lower frequency (delta, theta, alpha) and higher frequency (beta, gamma) EEG connectivity. The presence of brain injury and dysmaturation (low TMS scores and FA values) were both associated with increased high-frequency EEG connectivity, while immature white matter microstructure (low FA values) was associated with

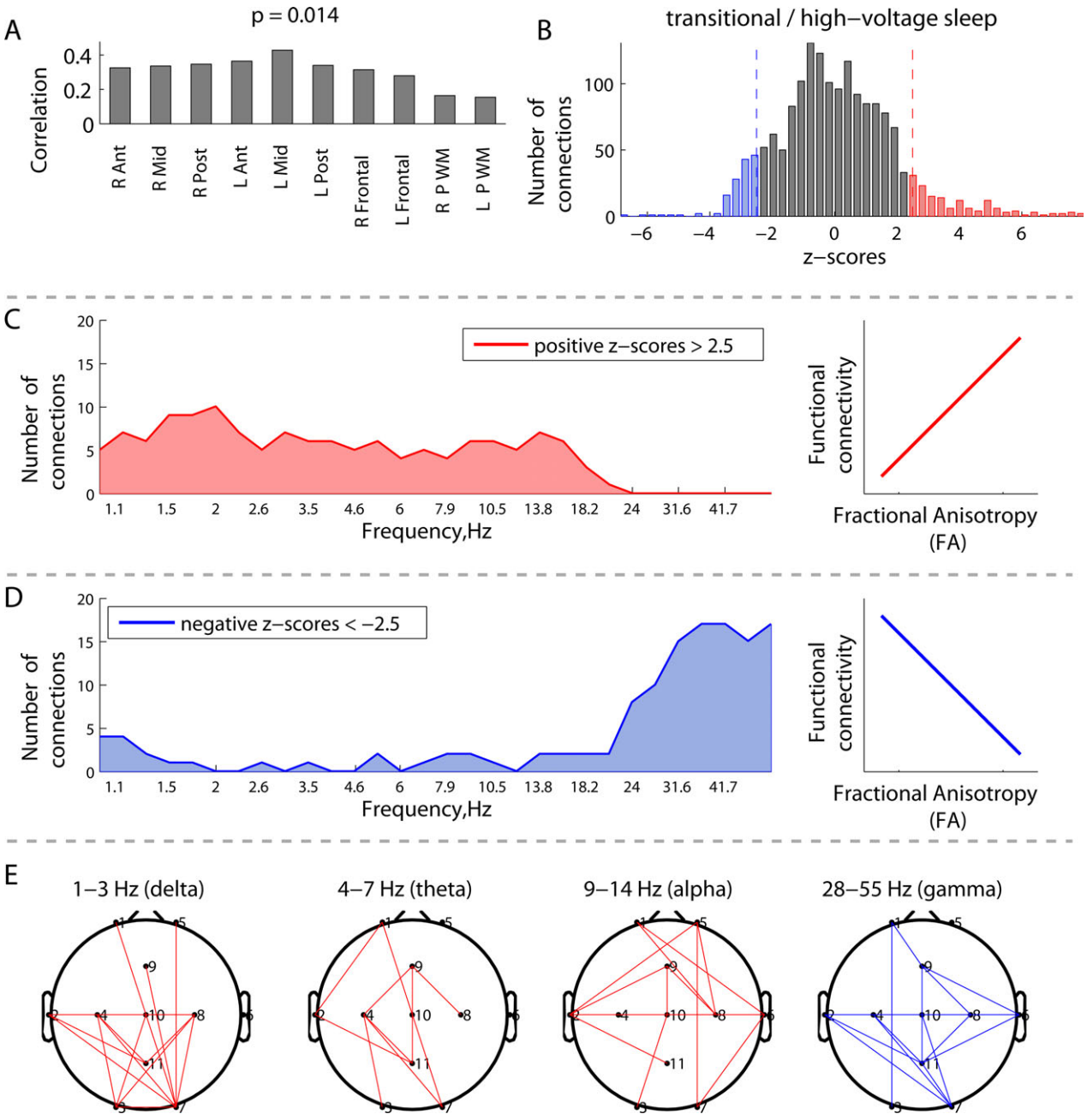

Figure 6. Correlations between EEG connectivity during transitional/high-voltage sleep and white matter fractional anisotropy (FA) (N = 11): (A) overall correlations between white matter FA at 10 specific regions of interest and EEG connectivity; (B) distribution of the z-scores, each associated with a unique combination of frequencies and connections, and showing the robustness of the latent variable in (A); (C and D) distribution of connections from the right (red) and left (blue) tails in (B) across frequencies, associated with robust positive and negative correlations between EEG connectivity and FA; (E) spatial distributions of the robust connections from the tails in (B) in the canonical frequency bands.

decreased low-frequency connectivity. Finally, the presence of brain injury was associated with significantly greater EEG background discontinuity.

EEG connectivity is understood to reflect synchronization of neural activity within and between distant cortical areas[20,24] requiring both structural and functional connections. Thalamo-cortical and cortico-cortical connections, which form the structural foundation of the synchronized cortical activity,[25] begin to develop during the second half of gestation[26] in parallel with profound maturational

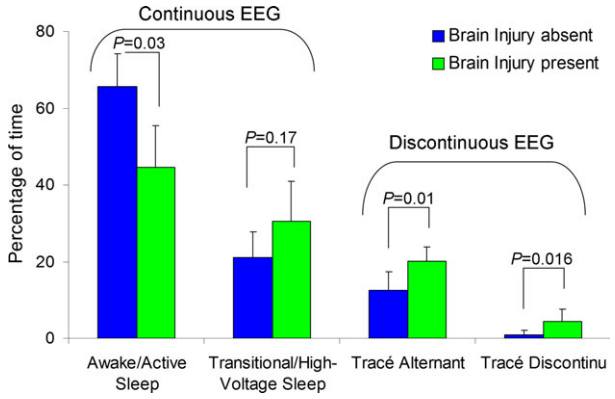

Figure 7. Composition of EEG background activity among subjects with (N = 5) and without brain injury (N = 15).

changes of EEG activity.[8] Developing structural connectivity should permit greater synchronization between brain regions, resulting in greater functional connectivity. However, the coordinated development of brain function likely requires selective changes in the dynamics of neurophysiological interactions among brain regions, rather than diffuse increases in connectivity. Indeed, both our present findings and several prior studies demonstrate such complex relationships between brain structure and function.

Given previous reports of delayed brain development in neonates with CHD (dysmaturation),[3,4] consistent with the encephalopathy of CHD,[27] we postulate that our observed increases in high-frequency connectivity and decreases in low-frequency connectivity, correlating with immature brain structure (low TMS) and microstructure (low FA), represent a maturational delay in functional brain networks. In fact, similar "dysmature" EEG findings have been reported in preterm neonates, specifically less low-frequency connectivity (delta, theta and alpha),[28–30] and greater high-frequency connectivity (beta and gamma)[30] than in term neonates. Alternatively, the observed changes in connectivity may relate more to brain injury itself. Given that brain injury and delayed brain development in neonates with CHD are closely intertwined, their relative contribution to EEG connectivity alterations cannot be differentiated within this relatively small cohort. In this respect, the absence of correlation between EEG connectivity and D_{av} in our cohort is not surprising. Brain immaturity and injury have been shown to exert opposite effects on D_{av}, associated with both increased[14,15] and decreased D_{av} levels,[31] respectively, thus confounding the association with EEG connectivity.

We focussed our connectivity analysis on continuous EEG activity because it reflects the establishment of mature patterns of communication within and between distant cortical regions,[25] and because connectivity analysis of discontinuous EEG activity is challenging. Immature pathways enable vertical synchronization of the topographically aligned thalamic and cortical neurons,[2] which is not well-suited to analysis using montages tangentially oriented to the cortical surface. However, emerging computational analysis methods could enable deeper understanding of the physiology underlying EEG discontinuity.[32]

Discontinuous EEG activity likely reflects transient thalamo-cortical pathways important for cortical development.[2,26] Due to the delayed brain development, these pathways might persist longer in CHD neonates. Indeed, our findings extend previous findings of abnormal background maturation as assessed by amplitude-integrated EEG,[9] by demonstrating increased EEG discontinuity on conventional EEG in CHD neonates with brain injury. Similarly, preterm neonates with brain injury have also been observed to display delays in functional maturation characterized by increased EEG discontinuity.[8,33,34] However, EEG discontinuity in our cohort was not related to structural and microstructural dysmaturation, which suggests that EEG connectivity is a more sensitive measure of functional maturation.

In the mature brain, low-frequency (delta, theta, alpha) and high-frequency (beta, gamma) EEG oscillations are thought to sustain different aspects of information flow. Low-frequency oscillations are thought to support global, distributed information processing and functional integration between distant cortical areas, while high-frequency oscillations are thought to support local processing of stimuli, segregation and differentiation within specialized cortical regions.[35] Hence, the observed decrease in connectivity at lower frequencies in neonates with CHD may signify weaker integration between distant cortical areas, while the increase in high-frequency connectivity may indicate stronger cortical differentiation. These observations could also be interpreted as the neurophysiological signature of a disruption in the natural "local to distributed" reorganization of spontaneous functional brain networks that begins early in development[36] and continues throughout childhood and adolescence.[37] Alternatively, the observed increase in high-frequency connectivity may signify an inability to desynchronize or reset the phases of local neural ensembles in response to global modulatory influences favoring large-scale integration.[38] We speculate that, at an early developmental stage, brain injury and brain dysmaturation in neonates with CHD disturb the fine tuning between the high- and low-frequency synchronization important for the establishment of neural networks and emergence of cognitive function. Thus, although our data do not reveal any specific topographic distribution, they suggest that EEG connectivity alterations in CHD neonates may be primarily expressed at a frequency level.

Several pathological mechanisms may be responsible for the link between impaired brain structure and function. Brain injury, particularly affecting the transient subplate zone, can disrupt both structural and functional network connectivity due to tissue loss.[39] The contribution of delayed structural and microstructural brain development to network dysfunction in neonates with CHD is less clear, but insights gained from studies of preterm neonates could be relevant. As in preterm neonates, chronic hypoxia due to CHD could mediate a maturational arrest of oligodendrocyte progenitors (preOL), leading to delayed myelination.[40] This abnormal myelination is known to disrupt neuronal network development via several mechanisms.[41,42] First, myelin determines conduction velocity, essential for ensuring the temporal coincidence of the synaptic inputs and the strengthening of connections.[43] In turn, functional activity promotes the development of myelin sheaths.[44] In addition, GABAergic interneurons, known to play a key role in the spatial and temporal organization of the developing cortical networks, are also harmed by perinatal hypoxia and could mediate the detrimental effects of CHD.[45] GABAergic interneurons have a central role in the development of perisomatic inhibition that underlies the emergence of mature gamma oscillatory activity.[2] Finally, the thalamus, one of the critical structures orchestrating neuronal EEG synchrony, is reduced in volume and shows neuronal loss and gliosis in neonates with CHD.[46,47]

An important question is whether these impairments in functional connectivity are transient or whether they persist and contribute to cognitive deficits later in life. Our data demonstrate that abnormal brain structure and microstructure in neonates with CHD correlate with an imbalance between frequency-dependent synchronization and desynchronization. At the network level, if we suppose that each EEG electrode represents a network node, we postulate that this imbalance reflects an inability to break the tight synchrony of local neural ensembles in the favor of large-scale integration of distributed neural populations. Longitudinal studies will be required to determine whether these disordered network properties are further exacerbated following cardiac surgery and persist into later life. Newly acquired brain injury has been described in around 40% of neonates after cardiac surgery.[5,6] However, these structural abnormalities, still visible on the anatomical MRI of teenaged survivors of TGA, were not associated with neurocognitive deficits.[48] Conversely, alterations in brain microstructure described in neonates,[4] continue to be observed in adolescents with CHD[49]; and white matter FA and regional brain volumes correlate with cognitive performance.[50,51] Moreover, white matter network topology is also altered in these adolescents, supporting our observations of a global alteration of distributed neuronal networks, which may mediate differences in ability observed across multiple neurocognitive domains.[52] Future research focussed on alterations in specific white-matter fiber pathways in infants with CHD utilizing DTI-based tractography methods would aid in assessing the developmental time course of disruptions in structural connectivity.

Our study has limitations. Although our findings indicate that neuronal network dysfunction among neonates with CHD is already present during early postnatal life, and correlates well with measures of structural and microstructural brain injury, longitudinal outcome data will be needed to establish whether the observed connectivity changes have long-lasting functional consequences. The 13-channel neonatal EEG montage used in this study provided insufficient spatial resolution to identify regional differences in EEG connectivity, which could be important for predicting developmental trajectories within specific neurocognitive domains. Some of the observed alterations in gamma-frequency connectivity may have been confounded by muscle artifact. To minimize this effect, we submitted to computational analysis only artifact-free epochs. Furthermore, because the observed EEG connectivity changes span multiple frequency bands, they are unlikely to be caused by muscle artifact. Scalp EEG measures may be contaminated by volume conduction, which has the potential to reveal spurious connectivity between brain regions.[24] However, volume conduction is known to be reduced in neonates,[53] and furthermore, we chose to apply wPLI to measure connectivity because of its resistance to contamination by volume conduction.[20] Finally, our observation of increased high-frequency connectivity could also reflect the persistence of early gamma oscillations mediated by excitatory thalamic inputs, which are known to synchronize local immature networks.[2] However, these transient gamma oscillations are a component of spontaneous activity transients, which occur during discontinuous EEG epochs and generally disappear by term age. Since our cohort comprised term or near-term neonates, and we performed our connectivity analyses on continuous EEG epochs, this phenomenon is less likely to explain our observed increase in gamma frequency connectivity. Finally, DTI measures were not obtained on preoperative MRIs of all neonates, however those with and without DTI measures performed had similar PMA, cardiac diagnoses, frequency of preoperative brain injury (27% vs. 29%, respectively) and TMS scores (13.7 ± 0.8 and 13.4 ± 0.9, respectively).

In conclusion, we demonstrate that, even before cardiac surgery, structural and microstructural brain abnormalities in neonates with CHD correlate with significant alterations in neuronal network function, manifesting as an imbalance between frequency-dependent synchronization

and desynchronization of local and distributed neural ensembles. Such early perturbations of developing neuronal networks, if sustained, may be responsible for the persistent neurocognitive impairment prevalent in adolescent survivors of CHD. These foundational insights into the complex interplay between evolving brain structure and function may have relevance for a wide spectrum of neurological disorders manifesting early developmental brain injury, and have translational potential to enhance the prediction of neurodevelopmental outcome.

Acknowledgments

We thank Patrick McQuillen for his critical appraisal of the manuscript. We are also thankful to Jean Gotman who helped with the data analysis by providing the Stellate-Harmonie Toolbox for MATLAB. This study was supported by the Canadian Institutes of Health Research (CIHR) Operating Grant to S. P. M. (MOP93780), as well as the CHU Sainte-Justine/Group Aldo scholarship and Detweiler Travelling Fellowship from the RCPSC (Royal College of Physicians and Surgeons of Canada) to A. B. S. P. M. is supported by the Bloorview Children's Hospital Chair in Paediatric Neuroscience.

Author Contributions

A. B., V. A. V., V. C., M. S., S. M. D., S. B., D. A. N., E. G. D., E. J. H., S. P. M. and C. D. H. were involved in the conception and design of the study. A. B., V. A. V., P. P., S. M., V. C., M. S., S. M. D., S. B., D. A. N., R. S., E. G. D., E. J. H., S. P. M. and C. D. H. acquired and analyzed the data. A. B. and V. A. V. prepared the first draft of the manuscript. All authors critically reviewed, edited, and approved the manuscript.

Conflict of Interest

None declared.

References

1. Smyser CD, Neil JJ. Use of resting-state functional MRI to study brain development and injury in neonates. Semin Perinatol 2015;39:130–140.
2. Colonnese M, Khazipov R. Spontaneous activity in developing sensory circuits: implications for resting state fMRI. Neuroimage 2012;62:2212–2221.
3. Licht DJ, Shera DM, Clancy RR, et al. Brain maturation is delayed in infants with complex congenital heart defects. J Thorac Cardiovasc Surg 2009;137:529–536.
4. Miller SP, McQuillen PS, Hamrick S, et al. Abnormal brain development in newborns with congenital heart disease. N Engl J Med 2007;357:1928–1938.
5. Beca J, Gunn JK, Coleman L, et al. New white matter brain injury after infant heart surgery is associated with diagnostic group and the use of circulatory arrest. Circulation 2013;127:971–979.
6. Dimitropoulos A, McQuillen PS, Sethi V, et al. Brain injury and development in newborns with critical congenital heart disease. Neurology 2013;81:241–248.
7. Bellinger DC, Wypij D, Rivkin MJ, et al. Adolescents with D-transposition of the great arteries corrected with the arterial switch procedure: neuropsychological assessment and structural brain imaging. Circulation 2011;124:1361–1369.
8. Lamblin MD, Andre M, Challamel MJ, et al. [Electroencephalography of the premature and term newborn. Maturational aspects and glossary]. Neurophysiol Clin 1999;29:123–219.
9. ter Horst HJ, Mud M, Roofthooft MT, et al. Amplitude integrated electroencephalographic activity in infants with congenital heart disease before surgery. Early Hum Dev 2010;86:759–764.
10. Williams IA, Tarullo AR, Grieve PG, et al. Fetal cerebrovascular resistance and neonatal EEG predict 18-month neurodevelopmental outcome in infants with congenital heart disease. Ultrasound Obstet Gynecol 2012;40:304–309.
11. Tokariev A, Videman M, Palva JM, et al. Functional brain connectivity develops rapidly around term age and changes between vigilance states in the human newborn. Cereb Cortex 2015;DOI:10.1093/cercor/bhv219
12. McQuillen PS, Hamrick SE, Perez MJ, et al. Balloon atrial septostomy is associated with preoperative stroke in neonates with transposition of the great arteries. Circulation 2006;113:280–285.
13. McQuillen PS, Barkovich AJ, Hamrick SE, et al. Temporal and anatomic risk profile of brain injury with neonatal repair of congenital heart defects. Stroke 2007;38:736–741.
14. Miller SP, Vigneron DB, Henry RG, et al. Serial quantitative diffusion tensor MRI of the premature brain: development in newborns with and without injury. J Magn Reson Imaging 2002;16:621–632.
15. Drobyshevsky A, Song SK, Gamkrelidze G, et al. Developmental changes in diffusion anisotropy coincide with immature oligodendrocyte progression and maturation of compound action potential. J Neurosci 2005;25:5988–5997.
16. Tsuchida TN, Wusthoff CJ, Shellhaas RA, et al. American clinical neurophysiology society standardized EEG terminology and categorization for the description of continuous EEG monitoring in neonates: report of the American Clinical Neurophysiology Society critical care monitoring committee. J Clin Neurophysiol 2013;30:161–173.
17. Delorme A, Makeig S. EEGLAB: an open source toolbox for analysis of single-trial EEG dynamics including

independent component analysis. J Neurosci Methods 2004;134:9–21.
18. Hosken JWJ. Ricker wavelets in their various guises. First Break 1988;6:24–33.
19. Auger F, Flandrin P, Gonçalvès P, Lemoine O. Time-frequency toolbox. http://tftb.nongnu.org/
20. Vinck M, Oostenveld R, van Wingerden M, et al. An improved index of phase-synchronization for electrophysiological data in the presence of volume-conduction, noise and sample-size bias. Neuroimage 2011;55:1548–1565.
21. Welch PD. The use of fast Fourier transform for the estimation of power spectra: a method based on time averaging over short, modified periodograms. IEEE Trans Audio Electroacoust 1967;15:70–73.
22. Krishnan A, Williams LJ, McIntosh AR, et al. Partial Least Squares (PLS) methods for neuroimaging: a tutorial and review. Neuroimage 2011;56:455–475.
23. McIntosh AR, Lobaugh NJ. Partial least squares analysis of neuroimaging data: applications and advances. Neuroimage 2004;23(suppl 1):S250–S263.
24. Nunez PL, Srinivasan R, Westdorp AF, et al. EEG coherency. I: statistics, reference electrode, volume conduction, Laplacians, cortical imaging, and interpretation at multiple scales. Electroencephalogr Clin Neurophysiol 1997;103:499–515.
25. Jones EG. Synchrony in the interconnected circuitry of the thalamus and cerebral cortex. Ann N Y Acad Sci 2009;1157:10–23.
26. Kostovic I, Judas M. The development of the subplate and thalamocortical connections in the human foetal brain. Acta Paediatr 2010;99:1119–1127.
27. Volpe JJ. Encephalopathy of congenital heart disease-destructive and developmental effects intertwined. J Pediatr 2014;164:962–965.
28. Duffy FH, Als H, McAnulty GB. Infant EEG spectral coherence data during quiet sleep: unrestricted principal components analysis–relation of factors to gestational age, medical risk, and neurobehavioral status. Clin Electroencephalogr 2003;34:54–69.
29. Gonzalez JJ, Manas S, De Vera L, et al. Assessment of electroencephalographic functional connectivity in term and preterm neonates. Clin Neurophysiol 2011;122:696–702.
30. Grieve PG, Isler JR, Izraelit A, et al. EEG functional connectivity in term age extremely low birth weight infants. Clin Neurophysiol 2008;119:2712–2720.
31. Ancora G, Testa C, Grandi S, et al. Prognostic value of brain proton MR spectroscopy and diffusion tensor imaging in newborns with hypoxic-ischemic encephalopathy treated by brain cooling. Neuroradiology 2013;55:1017–1025.
32. Koolen N, Dereymaeker A, Rasanen O, et al. Early development of synchrony in cortical activations in the human. Neuroscience 2016;322:298–307.
33. Ranasinghe S, Or G, Wang EY, et al. Reduced cortical activity impairs development and plasticity after neonatal hypoxia ischemia. J Neurosci 2015;35:11946–11959.
34. Benders MJ, Palmu K, Menache C, et al. Early brain activity relates to subsequent brain growth in premature infants. Cereb Cortex 2015;25:3014–3024.
35. Canolty RT, Knight RT. The functional role of cross-frequency coupling. Trends Cogn Sci 2010;14:506–515.
36. Smyser CD, Inder TE, Shimony JS, et al. Longitudinal analysis of neural network development in preterm infants. Cereb Cortex 2010;20:2852–2862.
37. Fair DA, Cohen AL, Power JD, et al. Functional brain networks develop from a "local to distributed" organization. PLoS Comput Biol 2009;5:e1000381.
38. Varela F, Lachaux JP, Rodriguez E, et al. The brainweb: phase synchronization and large-scale integration. Nat Rev Neurosci 2001;2:229–239.
39. Kostovic I, Kostovic-Srzentic M, Benjak V, et al. Developmental dynamics of radial vulnerability in the cerebral compartments in preterm infants and neonates. Front Neurol 2014;5:139.
40. Wellmann S, Buhrer C, Schmitz T. Focal necrosis and disturbed myelination in the white matter of newborn infants: a tale of too much or too little oxygen. Front Pediatr 2014;2:143.
41. Fields RD, Woo DH, Basser PJ. Glial regulation of the neuronal connectome through local and long-distant communication. Neuron 2015;86:374–386.
42. Nunez PL, Srinivasan R, Fields RD. EEG functional connectivity, axon delays and white matter disease. Clin Neurophysiol 2015;126:110–120.
43. Pajevic S, Basser PJ, Fields RD. Role of myelin plasticity in oscillations and synchrony of neuronal activity. Neuroscience 2014;276:135–147.
44. Wake H, Ortiz FC, Woo DH, et al. Nonsynaptic junctions on myelinating glia promote preferential myelination of electrically active axons. Nat Commun 2015;6:7844.
45. Robinson S, Li Q, Dechant A, et al. Neonatal loss of gamma-aminobutyric acid pathway expression after human perinatal brain injury. J Neurosurg 2006;104:396–408.
46. Kinney HC, Panigrahy A, Newburger JW, et al. Hypoxic-ischemic brain injury in infants with congenital heart disease dying after cardiac surgery. Acta Neuropathol 2005;110:563–578.
47. Owen M, Shevell M, Donofrio M, et al. Brain volume and neurobehavior in newborns with complex congenital heart defects. J Pediatr 2014;164:1121–1127.
48. Bellinger DC, Jonas RA, Rappaport LA, et al. Developmental and neurologic status of children after heart surgery with hypothermic circulatory arrest or low-flow cardiopulmonary bypass. N Engl J Med 1995;332:549–555.

49. Rivkin MJ, Watson CG, Scoppettuolo LA, et al. Adolescents with D-transposition of the great arteries repaired in early infancy demonstrate reduced white matter microstructure associated with clinical risk factors. J Thorac Cardiovasc Surg 2013;146:543–549.
50. Rollins CK, Watson CG, Asaro LA, et al. White matter microstructure and cognition in adolescents with congenital heart disease. J Pediatr 2014;165:936–944.
51. von Rhein M, Buchmann A, Hagmann C, et al. Brain volumes predict neurodevelopment in adolescents after surgery for congenital heart disease. Brain 2014;137: 268–276.
52. Panigrahy A, Schmithorst VJ, Wisnowski JL, et al. Relationship of white matter network topology and cognitive outcome in adolescents with D-transposition of the great arteries. Neuroimage Clin 2015;7:438–448.
53. Grieve PG, Emerson RG, Fifer WP, et al. Spatial correlation of the infant and adult electroencephalogram. Clin Neurophysiol 2003;114:1594–1608.

Supporting Information

Additional Supporting Information may be found online in the supporting information tab for this article:

Data S1. MRI protocol.
Data S2. EEG background patterns.
Data S3. Partial Least Squares analysis.

